Soft Matter

Increased Donnan Exclusion at High Salt Concentrations

Journal:	*Soft Matter*
Manuscript ID	SM-ART-10-2021-001511.R1
Article Type:	Paper
Date Submitted by the Author:	07-Dec-2021
Complete List of Authors:	Gao, Kevin; University of California Berkeley, Yu, Xiaopeng; University of California Berkeley Darling, Robert; Raytheon Technologies Research Center Newman, John; University of California Berkeley Balsara, Nitash; University of California, Chemical and Biomolecular Engineering

Increased Donnan Exclusion at High Salt Concentrations

Kevin W. Gao,[1,2,4] Xiaopeng Yu,[1,2] Robert M. Darling,[3,4] John Newman,[1] Nitash P. Balsara[*,1,2,4]

[1] *Department of Chemical and Biomolecular Engineering, University of California, Berkeley, CA 94720, USA*

[2] *Materials Sciences Division, Lawrence Berkeley National Lab, Berkeley, CA 94720, USA*

[3] *Raytheon Technologies Research Center, East Hartford, CT 06108, USA*

[4] *Joint Center for Energy Storage Research (JCESR), Argonne National Laboratory, Lemont, Illinois 60439, USA*

* Correspondence to: nbalsara@berkeley.edu

Abstract

The swelling of univalent and multivalent charged polymeric networks in electrolytic solutions is studied using a classical thermodynamic model. Such systems were first modeled by Donnan, who derived an expression for the chemical potential of the ions by introducing an electric potential that is commonly referred to as the Donnan potential. This well-established theory leads to a simple quadratic relationship for the partitioning of ions between the network and the external solution. When the concentration of fixed charges in the swollen gel is large enough, the electrolyte in the external solution is "excluded" from the gel (commonly referred to as Donnan exclusion). In the standard Donnan theory, and in virtually all subsequent theories, the magnitude of Donnan exclusion decreases with increasing electrolyte concentration in the external solution. Our model predicts this is not necessarily true; we show that the magnitude of Donnan exclusion increases with increasing electrolyte concentration over a broad range of parameter space (average chain length between crosslinks, fraction of charged monomers in the network, the nature of the interactions between the ions, solvent molecules and polymer chains, and ion concentration in the external solution). We also present explicit bounds for the validity of Donnan's original theory. Model predictions are compared to simulations and experimental data obtained for a cationic gel immersed in electrolytic solutions of salts containing univalent and bivalent cations.

Introduction

The partitioning of ionic species between a solution and a charged polymeric network is usually described by the term Donnan equilibrium.[1–3] This phenomenon, originally introduced in the context of physiology,[4–8] is important in several technological contexts[9,10] such as desalination and ion exchange resins. In the biological context, partitioning of ionic species into charged polymeric phases is important for the functioning of the lining of organs like the stomach and the colon[4–6] and assemblies of charged biomolecules such as proteins and RNA.[7,8]

The system of interest is illustrated in Figure 1. A charged gel with polymer strands comprising *N* repeat units between crosslinks is swollen in an ionic solution. The solution could contain an acid, a base, or a salt – we refer to this species as the electrolyte. For concreteness, we assume that the polymer has a fraction *f* of polymer repeat units that are negatively charged. We use volume fractions to describe the concentration of species (ions, polymer, and solvent). The standard result for partitioning of the electrolyte between the gel and solvent phases is:

$$\frac{\phi_-}{\phi^e_-} = -\frac{1}{2}\frac{\phi_{-,b}}{\phi^e_-} + \frac{1}{2}\sqrt{\left(\frac{\phi_{-,b}}{\phi^e_-}\right)^2 + 4} \qquad \#(1)$$

where ϕ_- and ϕ^e_- are the volume fractions of the free negative ions in the gel and external solution, respectively.[1] The volume fraction of the negative ions covalently bound to the polymer strands in the gel phase is $\phi_{-,b}$. Donnan exclusion refers to the regime wherein the ratio ϕ_-/ϕ^e_- is small, *i.e.*, the free ions are excluded from the gel. The use of concentration ratios in equation 1 minimizes the effect of the variable used to quantify ion concentrations. Molar concentrations are often used to describe Donnan equilibrium. In contrast, volume fractions are usually used in polymer physics; the molar concentration of polymer in the gel phase in Figure 1 is neither meaningful nor useful. We have thus chosen to use volume fractions in our analysis.

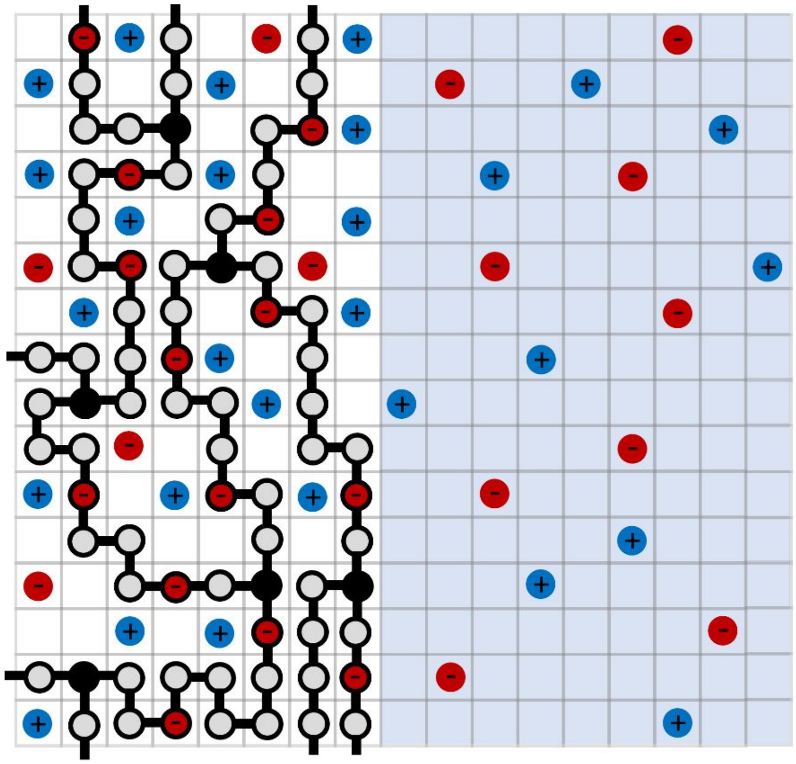

Figure 1. Schematic of a crosslinked polymer phase with negative charges covalently bound to the polymer chains in contact with a reservoir containing an electrolytic solution. Black circles represent crosslinks. The empty lattice sites are filled with solvent; solvent molecules are not shown explicitly for clarity. Some of the solvent molecules and ions in the electrolytic solution (shaded for clarity) enter the polymeric phase. The gel shown has $N = 9$ and $f = 2/9 = 0.22$.

Equation 1 predicts that ϕ_-/ϕ^e_- increases monotonically and smoothly approaches unity as the ion concentration in the external solution increases, *i.e.*, there is less Donnan exclusion with increasing external ion concentration. In previous theories on this subject,[11–14] separate thermodynamic models such as the Flory-Rehner theory[15] are used to determine $\phi_{-,b}$; equation 1 is assumed to apply regardless of the nature of ion-polymer interactions, solvent-polymer interactions, and the extent of crosslinking. Equation 1 is frequently used to describe swelling and ion partitioning in heterogeneous ionic polymers comprising solvophilic and solvophobic domains, wherein swelling due to uptake of solvent anions occurs exclusively in the solvophilic domains; the solvent is frequently water.

In Figure 2, we show swelling data obtained from a block copolymer containing charged polystyrenesulfonyllithium(trifluoromethylsulfonyl)imide (PSLiTFSI) chains equilibrated in an electrolytic mixture of ethylene carbonate (EC), dimethyl carbonate (DMC), and lithium bis(trifluoromethanesulfonyl)imide (LiTFSI) salt. The PSLiTFSI-*block*-polyethylene-*block*-PSLiTFSI (or PSLiTFSI-*b*-PE-*b*-PSLiTFSI) block copolymer was synthesized and characterized a recently submitted paper.[16] In Figure 2a, we show that total swelling, as quantified by the dependence of $\phi_{p,total}$, is a monotonic function of ϕ^e_-. In Figure 2b, we show the partitioning of the $TFSI^-$ anions in the solvophilic domains in the block copolymer as a function of the $TFSI^-$ anion volume fraction in the external solution. The noteworthy observation is that ϕ_-/ϕ^e_- does not increase monotonically and smoothly approach unity as the concentration of the external electrolyte solution is increased. In fact, ϕ_-/ϕ^e_- decreases slightly when ϕ^e_- is increased from 0.07 to 0.18.

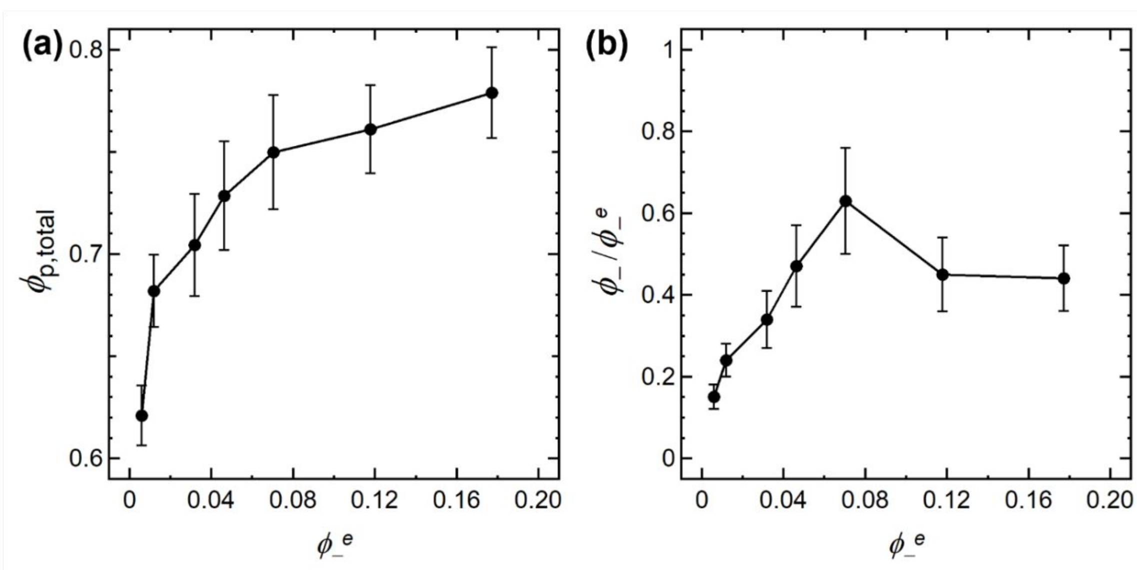

Figure 2. Experimental data for the swelling and salt partitioning between a PSLiTFSI-*b*-PE-*b*-PSLiTFSI triblock copolymer membrane and external solutions of LiTFSI in an EC/DMC mixture. (a) Swelling of the block copolymer, quantified by the total polymer volume fraction, $\phi_{p,total}$, as a function of the TFSI$^-$ anion volume fraction in the external solution, ϕ^e_-. (b) Dependence of the ratio of volume fraction of anions in the membrane to that in the external EC/DMC solution, ϕ_-/ϕ^e_-, on ϕ^e_-. Swelling is a monotonic function of ϕ^e_- but salt partitioning is not. Donnan exclusion increases with increasing salt concentration in the external solution in the $\phi^e_- > 0.07$ regime.

The question of what thermodynamic forces underly this behavior is difficult to address due to the complex interplay between morphology, chain deformation, and osmotic effects. As a first step toward answering this question, we sought to answer a much simpler question: what are the necessary ingredients for obtaining results that are qualitatively similar to the results shown in Figure 2. To answer this question, we present a simple model for the gel shown in Figure 1 based on Flory-Huggins theory[17–19] where the stretching of an ideal polymer network as quantified by the Flory-Rehner theory,[15] is incorporated directly into the framework originally developed by Donnan. Our approach is similar in spirit to those developed in ref [20] and [21] but differ significantly from approaches in many other recent theories[22,23] that use equation 1 as the primary governing equation. Consequently, regimes where the equilibrium properties of the gel deviate substantially from equation 1 are identified. We develop expressions that are applicable to symmetric (*e.g.,* $MgSO_4$) and asymmetric electrolytes (*e.g.,* $MgCl_2$).

Theory

We propose the following expression for the total Gibbs free energy change of mixing of the gel phase comprising the crosslinked polymer, electrolyte, and solvent molecules as shown in Figure 1 using the Flory-Huggins and Flory-Rehner theories:

$$\frac{\Delta G_m}{kT} = n\left[\frac{n_s}{n} ln\,(\phi_s) + \frac{n_+}{n} ln\,(\phi_+) + \frac{n_-}{n} ln\,(\phi_-) + \chi\frac{n_p}{n}(1-\phi_p)\right] + \frac{3n_p}{2N}\left(\phi_p^{-\frac{2}{3}} - 1\right) \#(2)$$

where n_i is the number of lattice sites occupied by each component, n is the total number of lattice sites, ϕ_i is the volume fraction of component i ($\phi_i = n_i/n$), and N is the number of polymer repeat units in each crosslinked strand.[15,17–19] The subscripts s, + and – stand for solvent, free cations, and free (unbound) anions in the gel, respectively. A fraction of the polymer repeat units f is negatively charged. Our model does not account for effects such as counterion condensation.[24,25] The first three terms on the right side of equation 2 represent entropic contributions and the fourth term represents the enthalpic contribution. χ is a lumped Flory-Huggins interaction parameter that quantifies the internal energy change of mixing between the polymer and all other species in the systems. This interaction parameter can be related to the individual interaction parameters between the constituents (see Equation S1 in the SI). The internal energy change of mixing solvent and electrolyte is ignored for simplicity. One can readily extend this approach to include separate parameters for the interaction between the solvent and polymer, the ions and polymer, and the ions and solvent. However, methods to evaluate multiple interaction parameters from typical experimental data have not yet been developed, and we thus present results as a function of a single χ parameter. The standard states are the pure components in the amorphous state; because pure ionic solids are often crystalline, the standard state may be hypothetical. The last term on the right side of equation 2 represents the deformation free energy of an ideal polymer network.[14,15] Following the Donnan approach, the expression for the free energy does not account for the charged nature of the phases of interest; both phases are, of course, electrically neutral.

The chemical potential of the species is given by:

$$\Delta\mu_i = \left(\frac{\partial \Delta G_m}{\partial m_i}\right)_{m_j, j \neq i} \#(3)$$

where m_i are the moles of species i; m_i=n_i/N_{AV}, and N_{AV} is Avogadro's number. Using equations 2 and 3, we get expressions for the chemical potential of the solvent and the ions in the gel:

$$\frac{\Delta\mu_S}{RT} = \ln(\phi_s) + \phi_p + \chi\phi_p^2 + \frac{\phi_p^{\frac{1}{3}}}{N}, \qquad \#(4)$$

$$\frac{\Delta\mu_+}{RT} = \ln(\phi_+) + \phi_p + \chi\phi_p^2 + \frac{\phi_p^{\frac{1}{3}}}{N}, \qquad \#(5)$$

$$\frac{\Delta\mu_-}{RT} = \ln(\phi_-) + \phi_p + \chi\phi_p^2 + \frac{\phi_p^{\frac{1}{3}}}{N}. \qquad \#(6)$$

Assuming that the solution in equilibrium with the gel is ideal, we obtain:

$$\frac{\Delta\mu_S^e}{RT} = \ln(\phi_s^e), \qquad \#(7)$$

$$\frac{\Delta\mu_+^e}{RT} = \ln(\phi_+^e), \qquad \#(8)$$

$$\frac{\Delta\mu_-^e}{RT} = \ln(\phi_-^e), \qquad \#(9)$$

where the superscript e stands for the external solution. Relaxing this assumption requires knowledge of activity coefficients, which are tabulated for many electrolytic solutions[26] but not for charged gels.

Equating the chemical potentials of the solvent in the two phases, we obtain:

$$\ln\left(\phi_s^e\right) = \ln\left(\phi_s\right) + \phi_p + \chi\phi_p^2 + \frac{\phi_p^{\frac{1}{3}}}{N}. \qquad \#(10)$$

The same approach cannot be used for the ions as the chemical potential of charged species depends on the electric field. This effect is accounted for by defining a potential U, and postulating an additive contribution to the chemical potentials of the ions as proposed by Donnan:

$$\ln\left(\phi^e_+\right) = \ln\left(\phi_+\right) + \phi_p + \chi\phi_p^2 + \frac{\phi_p^{\frac{1}{3}}}{N} + \frac{z_+FU}{RT} \qquad \#(11)$$

and

$$\ln\left(\phi^e_-\right) = \ln\left(\phi_-\right) + \phi_p + \chi\phi_p^2 + \frac{\phi_p^{\frac{1}{3}}}{N} + \frac{z_-FU}{RT}, \qquad \#(12)$$

where the charges numbers on the positive and negative ions are z_+ and z_-.[1] The charge numbers of the free and bound negative ions are assumed to be the same. The Donnan potential, which now contains elastic contributions, and can be thought of as a quasi-electrostatic potential as defined by Newman,[26] is introduced for computational purposes only. It cannot be measured; because the gel and solution phases in Figure 1 are at equilibrium, the electric potential difference between them measured with a suitable reference electrode is zero.[26,27]

Charge neutrality of the external solution implies:

$$\phi^e_+ = \frac{-z_-\phi^e_-}{z_+} \#(13)$$

Charge neutrality of the gel phase implies:

$$\phi_+ = \frac{-z_-}{z_+}(f\phi_p + \phi_-) \quad \#(14)$$

and

$$\phi_s = 1 - \left(1 - \frac{z_-}{z_+}f\right)\phi_p - \left(1 - \frac{z_-}{z_+}\right)\phi_- . \quad \#(15)$$

Eliminating *U* from equations 11 and 12 gives:

$$\ln\left((\phi^e_-)^{\left(\frac{1}{z_+}-\frac{1}{z_-}\right)}\left(\frac{-z_-}{z_+}\right)^{\frac{1}{z_+}}\right) = \ln\left((\phi^e_-)^{\frac{1}{z_+}}(\phi^e_+)^{\frac{1}{-z_-}}\right) + \left(\frac{1}{z_+} - \frac{1}{z_-}\right)\left(\phi_p + \chi\phi_p^2 + \frac{\phi_p^{\frac{1}{3}}}{N}\right) \quad \#(16)$$

which can be rewritten using equation 14 as:

$$\ln\left((\phi^e_-)^{\left(\frac{1}{z_+}-\frac{1}{z_-}\right)}\left(\frac{-z_-}{z_+}\right)^{\frac{1}{z_+}}\right) = \ln\left(\left(\frac{-z_-}{z_+}(f\phi_p + \phi_-)\right)^{\frac{1}{z_+}}(\phi_-)^{\frac{1}{-z_-}}\right) + \left(\frac{1}{z_+} - \frac{1}{z_-}\right)\left(\phi_p + \chi\phi_p^2 + \frac{\phi_p^{\frac{1}{3}}}{N}\right). \quad \#(17)$$

Equations 10 and 15 can be combined to give:

$$\ln\left(1 - \phi^e_-\left(1 - \frac{z_-}{z_+}\right)\right) = \ln\left(1 - \left(1 - \frac{z_-}{z_+}f\right)\phi_p - \left(1 - \frac{z_-}{z_+}\right)\phi_-\right) + \phi_p + \chi\phi_p^2 + \frac{\phi_p^{\frac{1}{3}}}{N}. \quad \#(18)$$

Equations 17 and 18 are the main results of our theory. Equation 17 arises due to equilibration of the free ions in the gel and the external solution while equation 18 arises from equilibration of the solvent between the two phases. For an electrolytic solution with a given value of ϕ^e_-, equations 17 and 18 can be solved simultaneously to determine the ion concentration in the gel, ϕ_-, and the extent of swelling quantified by ϕ_p, provided χ, *f,* and *N* are known. The Donnan potential may then be calculated using the following expression, which is based on equation 12:

$$U = \frac{RT}{z_- F}\left(\ln\left(\phi^e_-\right) - \ln\left(\phi_-\right) - \phi_p - \chi\phi_p^2 - \frac{\phi_p^{\frac{1}{3}}}{N}\right). \#(19)$$

For the case when both ϕ_p and ϕ_- are small, the logarithmic terms in the ionic equilibrium condition dominate, and equation 17 reduces to an algebraic equation,

$$\left(\frac{\phi_-}{\phi^e_-}\right)^{\left(\frac{1}{z_+} - \frac{1}{z_-}\right)}\left(\frac{f\phi_p}{\phi_-} + 1\right)^{\frac{1}{z_+}} - 1 = 0 \quad \#(20)$$

that can be solved for ϕ_- if *f,* ϕ_p and ϕ^e_- are known. Equation 20 is consistent with the treatment of multivalent Donnan equilibrium in ref. [11].

If $z_+ = -z_-$, equations 17, 18, and 20 reduce to:

$$\ln\left(\phi^e_-\right) = \frac{1}{2}\ln\left(\left(f\phi_p + \phi_-\right)\phi_-\right) + \phi_p + \chi\phi_p^2 + \frac{\phi_p^{\frac{1}{3}}}{N} \qquad \#(21)$$

and

$$\ln\left(1 - 2\phi^e_-\right) = \ln\left(1 - (1+f)\phi_p - 2\phi_-\right) + \phi_p + \chi\phi_p^2 + \frac{\phi_p^{\frac{1}{3}}}{N}, \quad \#(22)$$

and if both ϕ_p and ϕ_- are small, the logarithmic terms in the ionic equilibrium condition dominate, and equation 20 reduces to:

$$\frac{\phi_-}{\phi_-^e} = -\frac{1 f\phi_p}{2\phi_-^e} + \frac{1}{2}\sqrt{\left(\frac{f\phi_p}{\phi_-^e}\right)^2 + 4} = \frac{2}{\frac{f\phi_p}{\phi_-^e} + \sqrt{\left(\frac{f\phi_p}{\phi_-^e}\right)^2 + 4}} \#(23)$$

Equation 23 is identical to equation 1 because the bound ion concentration $\phi_{-,b}$is equal to $f\phi_p$. The second form of equation 23 avoids problems associated with subtracting two large numbers to obtain a small positive number, as is the case when the external solution becomes increasingly dilute.

Results and Discussion

The solution to equations 21 and 22 for $\chi = 1$ (the solvent and ions are poor solvents for the polymer) and $N = 10$ (a tightly crosslinked network) is shown in Figure 4, where ϕ_p and ϕ_- are plotted as a function of ϕ_-^e for a range of *f* values between 0.1 and 0.9. In Figure 4a, we see that gel swelling decreases (*i.e.*, ϕ_p increases) as ϕ_-^e increases. This is expected as interactions between the ions and polymer are unfavorable. Increasing the charge on the polymer, *f*, increases swelling at fixed ϕ_-^e due to the expected increase of free ions inside the gel. In Figure 4b, we see that the ratio ϕ_-/ϕ_-^e, which provides a measure of Donnan exclusion (low values of ϕ_-/ϕ_-^e indicate a greater extent of Donnan exclusion), increases monotonically with increasing ϕ_-^e, reaching a plateau that is a function of *f*. Increasing *f* results in decreased exclusion at fixed ϕ_-^e. One might have expected that increasing the charge on the polymer would lead to increased exclusion but the interplay between swelling and ionic interactions leads to the opposite conclusion.

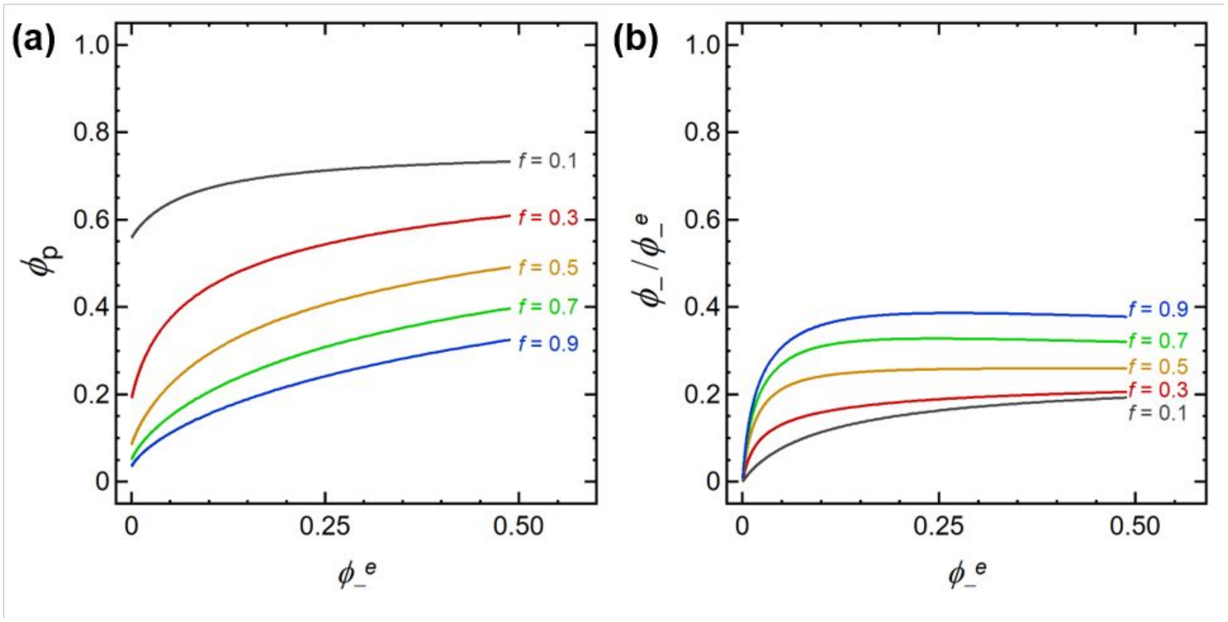

Figure 4. (a) Dependence of the polymer volume fraction in the gel phase, ϕ_p, on the volume fraction of anions in the external solution, ϕ^e_-. (b) Exclusion of ions in the gel: dependence of the ratio of volume fraction of anions in the gel to that in the external solution, ϕ_-/ϕ^e_-, on ϕ^e_-. Curves are shown for selected values of the fraction of charged monomers on the polymer strands, *f*. Parameters held fixed: $z_+ = -z_-$, $N = 10$, and $\chi = 1$.

Figure 5 shows results for $\chi = 1$ and $N = 50$ using the same format as Figure 4. The dependence of ϕ_p on ϕ^e_- is similar to that shown in Figure 4a: swelling reduces as ϕ^e_- increases. The dependence of ϕ_-/ϕ^e_- on ϕ^e_- is, however, non-monotonic for most of the values of *f* examined. Monotonic behavior is seen only at $f = 0.1$. For $f = 0.3$, for example, ϕ_-/ϕ^e_- increases with increasing ϕ^e_- in the dilute limit, reaches a maximum value of 0.373 at $\phi^e_- = 0.023$, before leveling off at 0.288 in the concentrated limit. The value of ϕ^e_- at the peak increases and the ϕ_-/ϕ^e_- peak broadens as *f* increases. Figure 6 shows results for $\chi = 1$ and $N =$

200. These results are qualitatively similar to Figure 5, except for the more pronounced maxima in the ϕ_{-}/ϕ^{e}_{-} versus ϕ^{e}_{-} curves. At $f = 0.1$, the maximum in ϕ_{-}/ϕ^{e}_{-} is followed by a shallow minimum before leveling off.

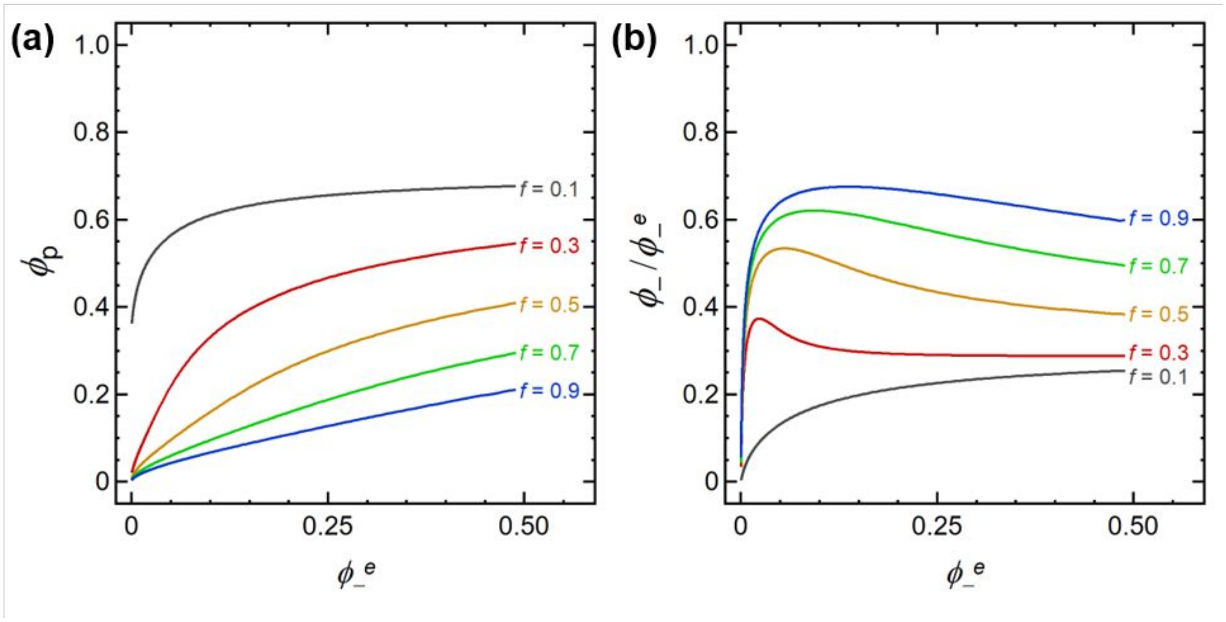

Figure 5. (a) Dependence of the polymer volume fraction in the gel phase, ϕ_p, on the volume fraction of anions in the external solution, ϕ^{e}_{-}. (b) Exclusion of ions in the gel: dependence of the ratio of volume fraction of anions in the gel to that in the external solution, ϕ_{-}/ϕ^{e}_{-}, on ϕ^{e}_{-}. Curves are shown for selected values of the fraction of charged monomers on the polymer strands, f. Parameters held fixed: $z_+ = -z_-$, $N = 50$, and $\chi = 1$.

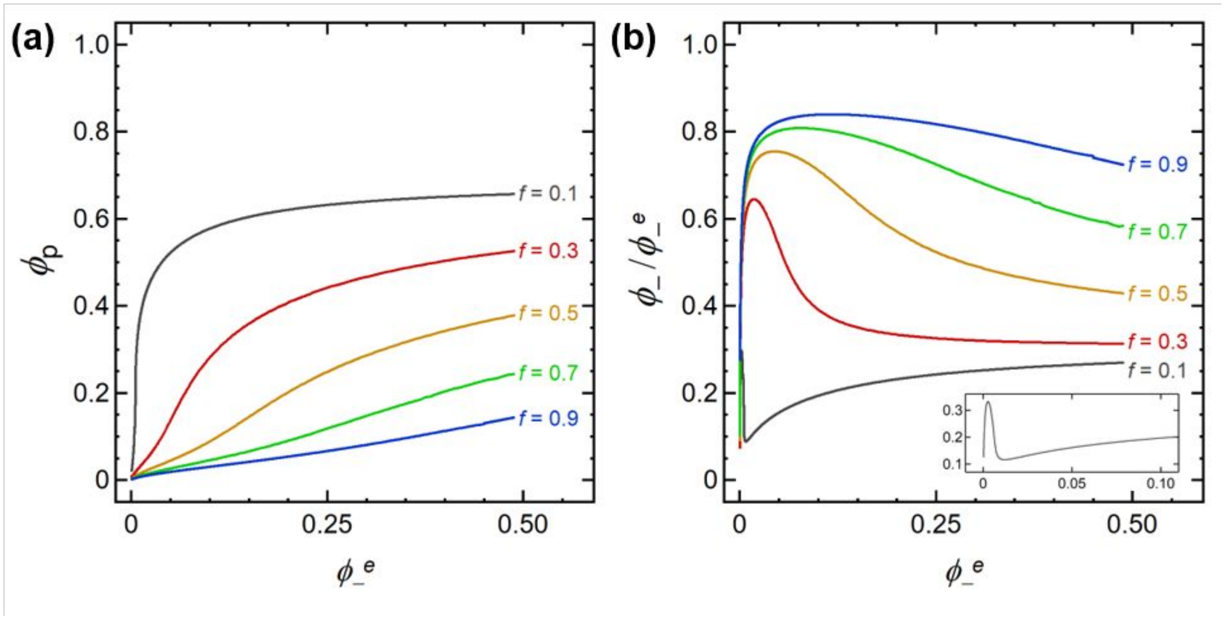

Figure 6. (a) Dependence of the polymer volume fraction in the gel phase, ϕ_p, on the volume fraction of anions in the external solution, ϕ^e_-. (b) Exclusion of ions in the gel: dependence of the ratio of volume fraction of anions in the gel to that in the external solution, ϕ_-/ϕ^e_-, on ϕ^e_-. Curves are shown for selected values of the fraction of charged monomers on the polymer strands, *f*. Parameters held fixed: $z_+ = -z_-$, $N = 200$, and $\chi = 1$. Inset shows $f = 0.1$ curve on an expanded scale for clarity.

Figure 7 shows the effect of changing χ on Donnan equilibrium at fixed values of $f = 0.3$ and $N = 50$. As seen in Figure 7a, the gels swell to greater extents as χ decreases from 1.5 to -1. At $\chi = -1$, the plateau value of ϕ_p is only 0.0728. The dependence of ϕ_-/ϕ^e_- on ϕ^e_- is monotonic only when $\chi \leq 0.5$. $\chi = 0.5$ represents the "theta condition" in polymer/solvent mixtures; this value of χ represents the border between favorable and unfavorable interactions between polymer segments and diluents. Significant Donnan exclusion at high concentrations is only seen when χ is greater than 0.5, as shown in Figure 7b. The non-monotonic dependence of ion exclusion in the gel arises from the competition between electrical effects which dominate at low values of ϕ^e_-, and thermodynamic interactions that are lumped into the χ parameter which dominate at high values of ϕ^e_-.

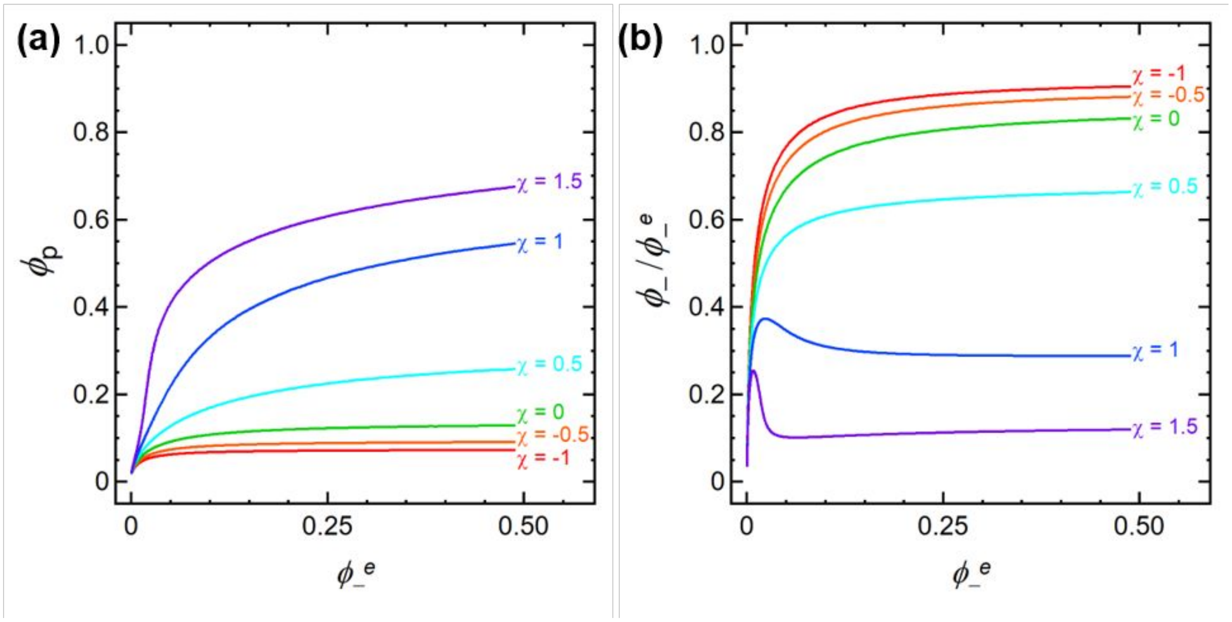

Figure 7. (a) Dependence of the polymer volume fraction in the gel phase, ϕ_p, on the volume fraction of anions in the external solution, ϕ^e_-. (b) Exclusion of ions in the gel: dependence of the ratio of volume fraction of anions in the gel to that in the external solution, ϕ_-/ϕ^e_-, on ϕ^e_-. Curves are shown for selected values of χ. Parameters held fixed: $z_+ = -z_-$, $N = 50$ and $f = 0.3$.

Figure 8a shows the effect of changing the charge on the ionic species at fixed f, N, and χ. In all cases, gel swelling decreases as ϕ^e_- increases. Increasing the charge on the bound and free negative ions (setting $z_- = -2$ but keeping $z_+ = +1$) results in increased swelling. This is expected because more positive ions are necessary in the gel to enforce charge neutrality. On the other hand, increasing the charge on the free positively charged ions (setting $z_+ = +2$ but keeping $z_- = -1$) results in decreased swelling, as expected. The extent of Donnan exclusion is non-monotonic in all cases, as shown in Figure 8b. The peak is less pronounced in the $z_+ = +2$ case compared to the $z_- = -2$ case. In the $z_+ = +2$ case, the maximum is followed by a shallow minimum, before ϕ_-/ϕ^e_- approaches a plateau. Regardless of the nature of the charged species, the plateau value of ϕ_-/ϕ^e_- is in the vicinity of 0.3.

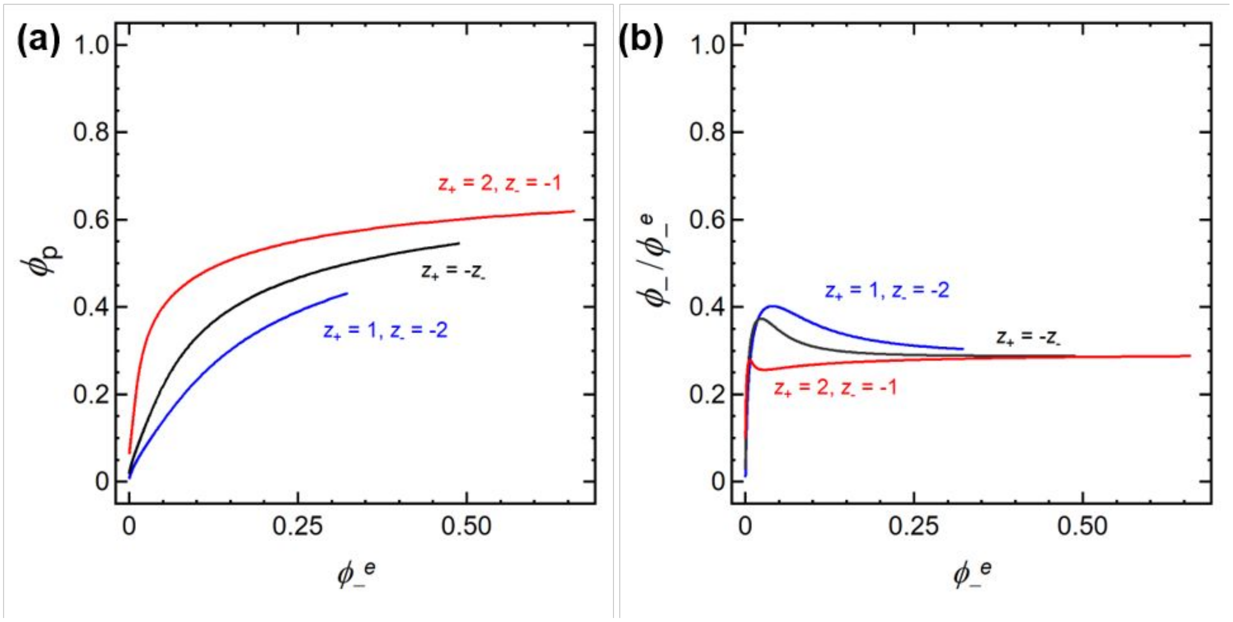

Figure 8. (a) Dependence of the polymer volume fraction in the gel phase, ϕ_p, on the volume fraction of anions in the external solution, ϕ_-^e. (b) Exclusion of ions in the gel: dependence of the ratio of volume fraction of anions in the gel to that in the external solution, ϕ_-/ϕ_-^e, on ϕ_-^e. Curves are shown for selected values of the charge numbers, z_+ and z_-. Parameters held fixed: $N = 50$ $\chi = 1$, and $f = 0.3$.

In Figure 9, we show the results of our calculations on a plot of ϕ_-/ϕ_-^e versus $\phi_{-,b}/\phi_-^e$ for three values of N, at fixed $f = 0.3$, $\chi = 1$, and $z_+ = z_-$. This format enables comparison of our results with that of Donnan; the dashed curve in Figure 9 represents equation 23. For $N = 10$, the results are qualitatively similar to the classical Donnan result but ϕ_-/ϕ_-^e is lower at all concentrations. Results for $N = 50$ and 200 obtained at sufficiently large values of $\phi_{-,b}/\phi_-^e$ are more-or-less coincident with the classical Donnan result. In this regime, using equation 23 as one of the governing equations is reasonable. The curves obtained for $N = 50$ and 200 at low values of $\phi_{-,b}/\phi_-^e \leq 2$, however, cannot be anticipated from the classical Donnan theory. The range of concentrations over which the classical Donnan result is a valid approximation depends on f, χ, N, and charge numbers. If we assume for concreteness that we are willing to accept an error of

10%, for N = 200, $\phi_{-,b}/\phi^{e}_{-}$, must be less than 0.74, and for N = 50, $\phi_{-,b}/\phi^{e}_{-}$, must be less than 3.3 (f = 0.3, χ = 1, and $z_+ = z_-$). The range of validity decreases rapidly with increasing N, and at N=10, there Donnan approximation is not valid over the entire $\phi_{-,b}/\phi^{e}_{-}$, range. For concreteness, we also show the dependence of $\phi_{-,b}$ on ϕ^{e}_{-} in the SI (see Figures S1-S5).

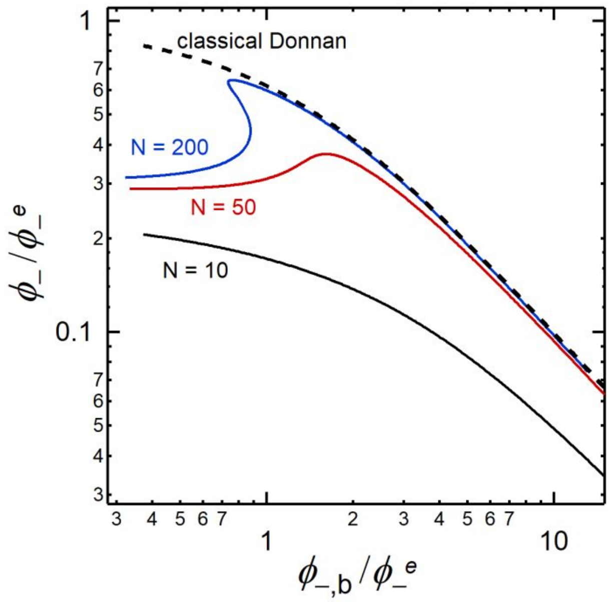

Figure 9. Comparing present theory with the classical Donnan prediction. Dependence of the ratio of volume fraction of anions in the gel to that in the external solution, ϕ_{-}/ϕ^{e}_{-}, on the ratio of covalently bound anion volume fraction in the gel to that in the external solution, $\phi_{-,b}/\phi^{e}_{-}$. Dashed curve is the classical Donnan prediction, equation 23. Curves are shown for selected values of N. Parameters held fixed in the solid curves: $z_+ = -z_-$, $\chi = 1$, and $f = 0.3$. Each curve is a parametric plot wherein ϕ^{e}_{-} is varied from 0.007 to 0.49. The dependence of $\phi_{-,b}$ on ϕ^{e}_{-} is given in the SI.

Figures 5-8 demonstrate that Donnan exclusion can increase as the electrolyte concentration in the external solution increases over a broad range of parameter space (average chain length between crosslinks, fraction of charged monomers in the network, the nature of the interactions between the ions, solvent molecules and polymer chains, and ion concentration in the external solution). This conclusion was not evident in previous theoretical and experimental studies,[20,22,23,28–30] including theories that are similar in spirit to the theory presented here (*e.g.*, ref. [20]). The only example of increasing Donnan exclusion with increasing electrolyte concentration in the external solution is reported in computer simulations of ionic gel swelling, reported in ref. [31].

We use the framework described above to qualitatively understanding the salt partitioning results obtained in swollen the PSLiTFSI-*b*-PE-*b*-PSLiTFSI block copolymer discussed in Figure 2. Before we begin a quantitative analysis, it is important note that there are many parameter sets that give results that are qualitatively similar to Figure 2; in Figures 5 and 6 we see many examples where ϕ_p is a monotonically increasing function of ϕ^e_- as is the case in Figure 5a, but ϕ_-/ϕ^e_- first increases with increasing ϕ^e_- but ultimately decreases with increasing ϕ^e_- in the high salt concentration regime. Yet such behavior is seldom reported in the theoretical and experimental literature on Donnan equilibrium.[11–14,32–36]

The quantitative data set obtained from our experimental system is provided in the SI. The total polymer volume fraction of the gel phase, $\phi_{\mathrm{p,total}}$, was calculated from the following equation:

$$\phi_{\mathrm{p,total}} = \frac{\dfrac{1}{\rho_p}}{\left(\dfrac{1}{\rho_p} + \dfrac{W_e}{\rho_e}\right)}, \#(24)$$

where ρ_p is the density of the PSLiTFSI-*b*-PE-*b*-PSLiTFSI triblock copolymer ($\rho_p = 1.06\frac{g}{cm^3}$), W_e is the external EC/DMC/LiTFSI solution uptake in grams, and ρ_e is the density of the external solution in grams cm^{-3}. The polymer volume fraction of the charged PSLiTFSI-rich microphase only, ϕ_p, was estimated using the following equation and neglecting volume changes of mixing:

$$\phi_p = \phi_{\mathrm{p,total}}\left(\frac{\frac{2M_{PSLiTFSI}}{\rho_{PSLiTFSI}}}{\frac{M_{PE}}{\rho_{PE}} + \frac{2M_{PSLiTFSI}}{\rho_{PSLiTFSI}}}\right), \#(25)$$

where M_i and ρ_i are the molecular weight and density of block i in the triblock copolymer respectively ($M_{PSLiTFSI} = 10\frac{\mathrm{kg}}{\mathrm{mol}}$, $M_{PE} = 50\frac{\mathrm{kg}}{\mathrm{mol}}$; $\rho_{PSLiTFSI} = 1.57\frac{\mathrm{g}}{\mathrm{cm}^3}$, $\rho_{PE} = 0.94\frac{\mathrm{g}}{\mathrm{cm}^3}$). The external anion volume fraction, ϕ^e_-, was calculated from the following equation:

$$\phi^e_- = \frac{1}{2}\left(\frac{\frac{m\rho_s V_{LiTFSI}}{1000}}{\frac{m\rho_s V_{LiTFSI}}{1000} + 1}\right), \#(26)$$

where m is the molality of the external salt solution, ρ_s is the density of the EC/DMC solvent, and V_{LiTFSI} is the molar volume of LiTFSI ($V_{LiTFSI} = 99\frac{\mathrm{cm}^3}{\mathrm{mol}}$).[37]

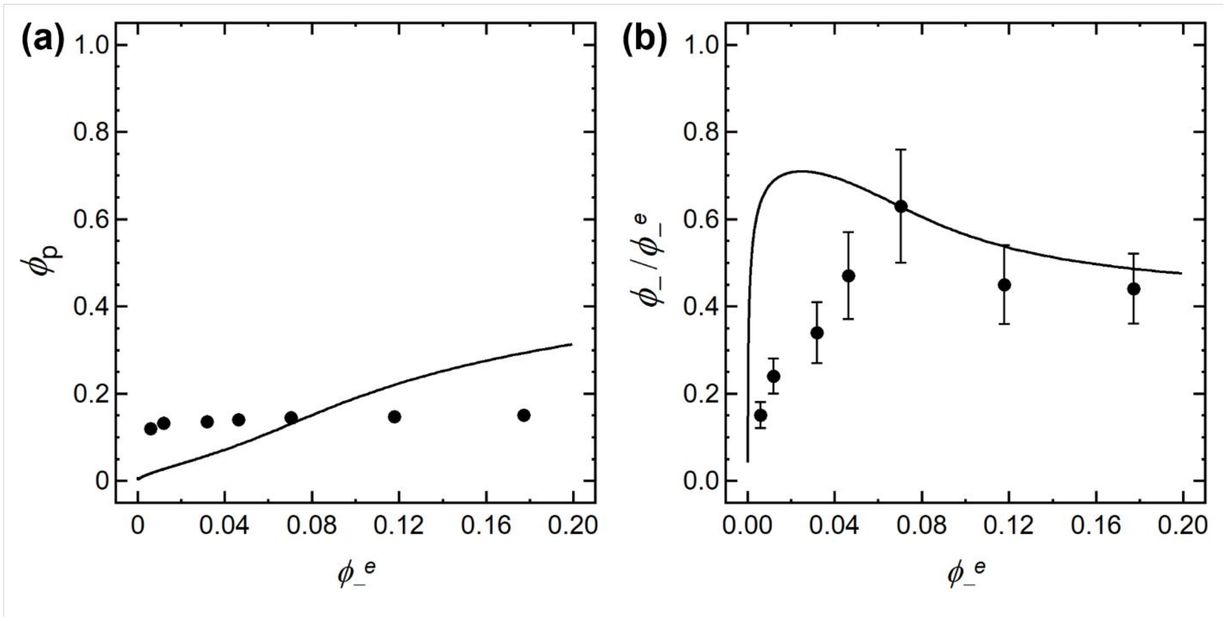

Figure 10. Experimental data for the swelling and salt partitioning between a PSLiTFSI-*b*-PE-*b*-PSLiTFSI triblock copolymer membrane and external solutions of LiTFSI in an EC/DMC mixture. (a) Dependence of the polymer volume fraction of the electrolyte-rich microphase, ϕ_p, on the volume fraction of anions in the external solution, ϕ^e_-. (b) Exclusion of ions in the gel: dependence of the ratio of volume fraction of anions in the gel to that in the external solution, ϕ_-/ϕ^e_-, on ϕ^e_-. Curves were calculated using $\chi = 0.85$, $z_+ = -z_-$, $N = 250$ and $f = 0.3$.

In Figure 10 we compare the experimental data with theoretical predictions for a particular set of parameters ($\chi = 0.85$, $z_+ = -z_-$, $N = 250$ and $f = 0.3$). It is evident that our simple model is in qualitative agreement with the experimental observations. We do not expect quantitative agreement because our theory does not address microphase separation, among other complexities beyond the scope of this work. These complexities include counterion condensation, non-ideality of mixing that is beyond Flory-Huggins theory, and the fact that the model used to quantify swelling does not account for the presence of charges.

We also compare the predictions of our theory with experimental data on the partitioning of NaCl and $MgCl_2$ in a negatively charged polymer network taken from the literature.[36] In

Figure 11, we show the dependence of ϕ_p and ϕ_-/ϕ^e_- on ϕ^e_- for the two systems. These parameters were obtained from the data reported in ref. [36] using the following relationships:

$$\phi_p = \frac{\frac{1}{\rho_p}}{\left(\frac{1}{\rho_p} + \frac{W_u}{\rho_w} + v_- \frac{C_- W_u V_-}{1000} + v_+ \frac{C_+ W_u V_+}{1000}\right)}, \#(27)$$

$$\phi_- = \frac{v_- \frac{C_- W_u V_-}{1000}}{\left(\frac{1}{\rho_p} + \frac{W_u}{\rho_w} + v_- \frac{C_- W_u V_-}{1000} + v_+ \frac{C_+ W_u V_+}{1000}\right)}, \#(28)$$

$$\phi^e_- = v_- \frac{C_e V_-}{1000}, \#(29)$$

where ρ_p is the density of the dry polymer network ($\rho_p = 1.40 \frac{\text{g}}{\text{cm}^3}$), ρ_w is the density of water ($\rho_w = 1.00 \frac{\text{g}}{\text{cm}^3}$), W_u is the water uptake in grams (Figure 4a in ref. [36]), v_- and v_+ are the stoichiometric coefficients of the free anion (Cl^-) and cation (Na^+ or Mg^{2+}) respectively, C_- and C_+ are the concentrations of the free anions and cations in moles per liter in the gel phase (Figures 6-8 in ref. [36]), V_- and V_+ are the molar volumes of the anion ($V_- = V_{Cl^-} = 27.21 \frac{\text{cm}^3}{\text{mol}}$, ref. [38]) and cation ($V_+ = V_{Na^+} = 1.94 \frac{\text{cm}^3}{\text{mol}}$; $V_+ = V_{Mg^{2+}} = 20.97 \frac{\text{cm}^3}{\text{mol}}$, ref. [38]), and C_e is the electrolyte concentration in the external solution in moles per liter (Figures 6-7 in ref. [36]). Each term in equations 27 and 28 represents the volume occupied by one of the constituents in the system: the denominator is the total volume composed of the volumes of polymer, water uptake, anions, and cations, respectively. We assume additive volumes and note that equations 27 and 28 are derived using 1 gram weight of dry polymer as the basis. There are no widely accepted values for the molar volumes of individual ions; the values reported in ref. [38] that we have used are based on simulations while a different approach based on ion transport parameters is presented in ref. [39] (transport parameters for multivalent salts have not yet been determined).

The data in Figure 11 are in qualitative agreement with the theory. Both the extent of swelling and Donnan exclusion are lower for $MgCl_2$ ($z_+ = +2$ and $z_- = -1$) compared to NaCl ($z_+ = -z_-$). The curves through the data in Figure 11 represent theoretical predictions with $N = 9$, $f = 0.1$, $\chi = 0.65$ for NaCl and $\chi = 0.52$ for $MgCl_2$. Our objective here is not to suggest that the present theory is more accurate than those previously described[11–14,32–36] in the field; the main point of Figure 11 is that the present theory appears to be a reasonable starting point for studying the partitioning of electrolytes into charged gels. More work is needed to study the variety of regimes predicted by our theory.

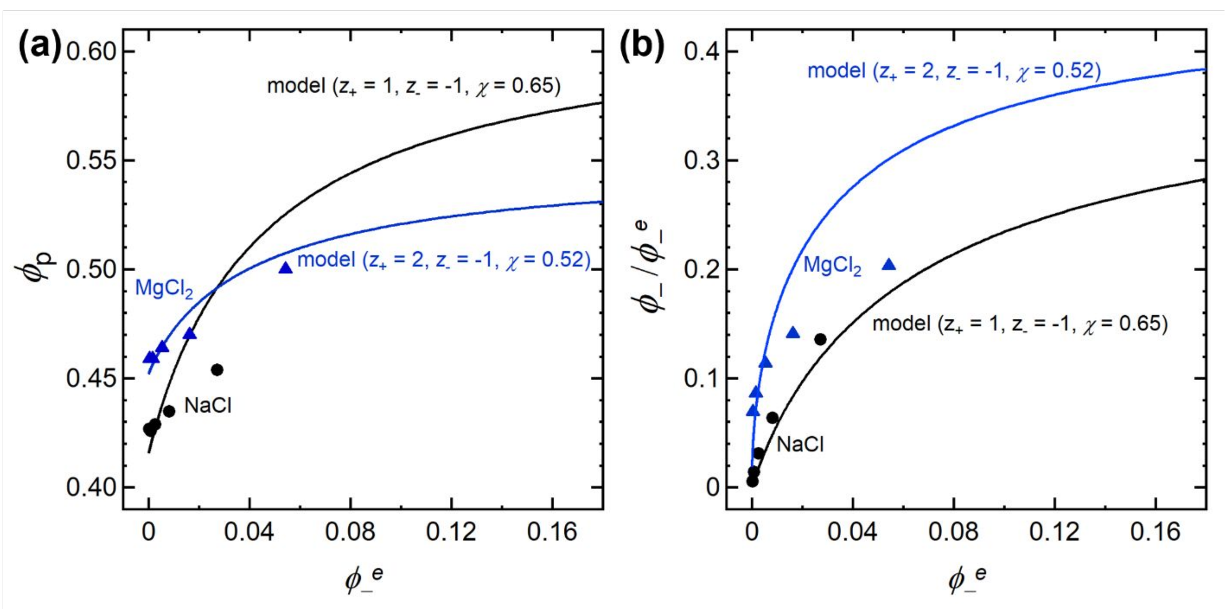

Figure 11. Comparing experimental data from ref. 36 with theoretical predictions. Data points represent partitioning of NaCl and $MgCl_2$ from an aqueous solution into an acrylamide-based polymeric gel with sulfonic acid groups. (a) Dependence of the polymer volume fraction in the gel phase, ϕ_p, on the volume fraction of anions in the external solution, ϕ^e_-. (b) Exclusion of ions in the gel: dependence of the ratio of

volume fraction of anions in the gel to that in the external solution, ϕ_{-}/ϕ^{e}_{-}, on ϕ^{e}_{-}. Curves were calculated using $\chi = 0.65$ and $z_{+} = -z_{-}$ for comparisons with the NaCl data, and $\chi = 0.52$, $z_{+} = 2$ and $z_{-} = -1$ for comparisons with the $MgCl_2$ data. Parameters held fixed: $N = 9$ and $f = 0.1$.

Conclusion

We present a new set of equations for describing Donnan equilibrium – the partitioning of ions between a charged gel and an electrolytic solution that accounts for the elasticity of the gel. The original Donnan theory accounts for ion interactions and correctly predicts that when the ion concentration in the external liquid ϕ^{e}_{-} is sufficiently low, they are excluded from the gel. Our main accomplishment is to combine Donnan's original approach with a rudimentary model that accounts for the free energy changes associated with gel swelling. The original quadratic equation is replaced by two coupled algebraic equations that must be solved to self-consistently predict both gel swelling, as quantified by ϕ_p, and Donnan exclusion, as quantified by ϕ_{-}/ϕ^{e}_{-}. Our analysis applies to both univalent and multivalent ions. We present limited comparisons of our predictions with experimental data, noting that substantial work is required to compare experimental data with predictions based on independently determined model parameters (χ, f, and N).

Conflict of Interest

The authors declare no competing financial interest.

Supplementary Information

(a) Synthesis, characterization, and measurement of electrolyte uptake and salt partitioning of PSLiTFSI-*b*-PE-*b*-PSLiTFSI. (b) Swelling data given in table form. (c) A more general expression for the free energy of mixing accounting for different interaction parameters is presented. (d) The bound ion concentration in the gel, $\phi_{-,b}$, is shown explicitly as a function of ϕ^e_- for the systems examined in Figures 4-8. (e) The comparison between model predictions and experimental data shown in Figures 10b and 11b are replotted using solvent and ion concentrations in mol/L.

Acknowledgements

This work was intellectually led by the Joint Center for Energy Storage Research (JCESR), an Energy Innovation Hub funded by the U.S. Department of Energy, Office of Science, Office of Basic Energy Science, under Contract No. DE-AC02-06CH11357, which supported work done by K.W.G. and X.P. under the supervision of N.P.B and R.M.D. K.W.G. acknowledges funding from a National Defense and Science Engineering Graduate Fellowship. We thank Benny Freeman for stimulating discussions.

List of Symbols

N	number of repeat units between crosslinks
f	fraction of charged monomers in the gel phase
ϕ_i	volume fraction of component *i* in the gel phase
ϕ_i^e	volume fraction of component *i* in the external solution phase

$\phi_{-,b}$	volume fraction of the bound negative ions in the gel phase
$\phi_{\mathrm{p,total}}$	total polymer volume fraction of gel phase after swelling
ΔG_m	Gibbs free energy of mixing
k	Boltzmann constant
T	absolute temperature
n_i	number of lattice sites occupied by component i
n	total number of lattice sites
χ	Flory-Huggins interaction parameter
μ_i	chemical potential of species i
m_i	moles of species i
N_{AV}	Avogadro's number
R	molar gas constant
z_+	charge number of positive ion
z_-	charge number of negative ion
F	Faraday constant
U	Donnan potential
ρ_i	density of component i
W_e	external solution uptake
M_i	molecular weight of component i
m	molality
V_i	intrinsic molar volume of species i
W_u	water uptake
v_i	stoichiometric coefficient of ion i

C_i	concentration of species *i* in the gel phase
C_e	anion concentration of external solution

References

(1) Donnan, F. G. Theorie Der Membrangleichgewichte Und Membranpotentiale Bei Vorhandensein von Nicht Dialysierenden Elektrolyten. Ein Beitrag Zur Physikalisch-Chemischen Physiologie. *Zeitschrift fur elektrochemie* **1911**, *17* (10), 572–581. https://doi.org/10.1002/bbpc.19110171405.

(2) Donnan, F. G. The Theory of Membrane Equilibria. *Chem. Rev.* **1924**, *1*, 73–90. https://doi.org/10.1021/cr60001a003.

(3) Donnan, F. G. Theory of Membrane Equilibria and Membrane Potentials in the Presence of Non-Dialysing Electrolytes. A Contribution to Physical-Chemical Physiology. *J. Memb. Sci.* **1995**, *100* (1), 45–55. https://doi.org/10.1016/0376-7388(94)00297-C.

(4) Katchalsky, A.; Kedem, O. Thermodynamics of Flow Processes in Biological Systems. *Biophys. J.* **1962**, *2* (2), 53–78. https://doi.org/10.1016/s0006-3495(62)86948-3.

(5) Bansil, R.; Stanley, E.; Thomas LaMont, J. Mucin Biophysics. *Annu. Rev. Physiol.* **1995**, *57* (February), 635–657. https://doi.org/10.1146/annurev.ph.57.030195.003223.

(6) Preska Steinberg, A.; Wang, Z. G.; Ismagilov, R. F. Food Polyelectrolytes Compress the Colonic Mucus Hydrogel by a Donnan Mechanism. *Biomacromolecules* **2019**, *20* (7), 2675–2683. https://doi.org/10.1021/acs.biomac.9b00442.

(7) Mussel, M.; Basser, P. J.; Horkay, F. Ion-Induced Volume Transition in Gels and Its Role in Biology. *Gels* **2021**, *7* (1), 1–17. https://doi.org/10.3390/GELS7010020.

(8) Yewdall, N. A.; André, A. A. M.; Lu, T.; Spruijt, E. Coacervates as Models of Membraneless Organelles. *Curr. Opin. Colloid Interface Sci.* **2021**, *52*, 101416.

https://doi.org/10.1016/j.cocis.2020.101416.

(9) Helfferich, F. *Ion Exchange*; McGraw-Hill: New York, 1962.

(10) Schlenoff, J. B.; Yang, M.; Digby, Z. A.; Wang, Q. Ion Content of Polyelectrolyte Complex Coacervates and the Donnan Equilibrium. *Macromolecules* **2019**, *52* (23), 9149–9159. https://doi.org/10.1021/acs.macromol.9b01755.

(11) Gehrke, S. H. Kinetics of Gel Volume Change and Its Interaction with Solutes, University of Minnesota, 1986.

(12) Skouri, R.; Schosseler, F.; Munch, J. P.; Candau, S. J. Swelling and Elastic Properties of Polyelectrolyte Gels. *Macromolecules* **1995**, *28* (1), 197–210. https://doi.org/10.1021/ma00105a026.

(13) Geise, G. M.; Falcon, L. P.; Freeman, B. D.; Paul, D. R. Sodium Chloride Sorption in Sulfonated Polymers for Membrane Applications. *J. Memb. Sci.* **2012**, *423–424*, 195–208. https://doi.org/10.1016/j.memsci.2012.08.014.

(14) Doi, M. *Soft Matter Physics*; Oxford University Press: New York, 2013.

(15) Flory, P. J.; Rehner, J. Statistical Mechanics of Cross-Linked Polymer Networks I. Rubberlike Elasticity. *J. Chem. Phys.* **1943**, *11* (11), 512–520. https://doi.org/10.1063/1.1723791.

(16) Yu, X.; Jiang, X.; Seidler, M. E.; Shah, N. J.; Gao, K. W.; Chakraborty, S.; Villaluenga, I.; Balsara, N. P. Ionic Separator Formed by Block Copolymer Microphase Separation: A Gateway for Alleviating Concentration Polarization in Batteries. Submitted.

(17) Flory, P. J. Thermodynamics of High Polymer Solutions. *J. Chem. Phys.* **1941**, *9*, 660.

https://doi.org/10.1063/1.1750971.

(18) Flory, P. J. Thermodynamics of High Polymer Solutions. *J. Chem. Phys.* **1942**, *46* (15), 51–61. https://doi.org/10.1063/1.1723621.

(19) Huggins, M. L. Some Properties of Solutions of Long-Chain Compounds. *J. Phys. Chem.* **1942**, *46* (1), 151–158. https://doi.org/10.1021/j150415a018.

(20) Katchalsky, A.; Michaeli, I. Polyelectrolyte Gels in Salt Solutions. *J. Polym. Sci.* **1955**, *15* (79), 69–86. https://doi.org/10.1002/pol.1955.120157906.

(21) Khokhlov, A. R.; Dormidontova, E. E. Self-Organization in Ion-Containing Polymer Systems. *Phys.-Usp.* **1997**, *40* (2), 109–124. https://doi.org/10.1070/PU1997v040n02ABEH000191.

(22) Rička, J.; Tanaka, T. Swelling of Ionic Gels: Quantitative Performance of the Donnan Theory. *Macromolecules* **1984**, *17* (12), 2916–2921. https://doi.org/10.1021/ma00142a081.

(23) Jeon, C. H.; Makhaeva, E. E.; Khokhlov, A. R. Swelling Behavior of Polyelectrolyte Gels in the Presence of Salts. *Macromol. Chem. Phys.* **1998**, *199* (12), 2665–2670. https://doi.org/10.1002/(SICI)1521-3935(19981201)199:12<2665::AID-MACP2665>3.0.CO;2-6.

(24) Manning, G. S. Polyelectrolytes. *Annu. Rev. Phys. Chem.* **1972**, *23*, 117–140. https://doi.org/10.1146/annurev.pc.23.100172.001001.

(25) Manning, G. S. Limiting Laws and Counterion Condensation in Polyelectrolyte Solutions II. Self-Diffusion of the Small Ions. *J. Chem. Phys.* **1969**, *51* (3), 934–938. https://doi.org/10.1063/1.1672158.

(26) Newman, J.; Balsara, N. P. *Electrochemical Systems*, 4th ed.; John Wiley & Sons, Inc.: Hoboken, New Jersey, 2020.

(27) Vis, M.; Peters, V. F. D.; Tromp, R. H.; Erné, B. H. Donnan Potentials in Aqueous Phase-Separated Polymer Mixtures. *Langmuir* **2014**, *30* (20), 5755–5762. https://doi.org/10.1021/la501068e.

(28) Khokhlov, A. R.; Starodubtzev, S. G.; Vasilevskaya, V. V. *Conformational Transitions in Polymer Gels: Theory and Experiment*; 1993; Vol. 109. https://doi.org/10.1007/3-540-56791-7_3.

(29) Kramarenko, E. Y.; Philippova, O. E.; Khokhlov, A. R. Polyelectrolyte Networks as Highly Sensitive Polymers. *Polym. Sci. - Ser. C* **2006**, *48* (1), 1–20. https://doi.org/10.1134/S1811238206010012.

(30) Khokhlov, A. R.; Kramarenko, E. Y.; Makhaeva, E. E.; Starodubtzev, S. G. Collapse of Polyelectrolyte Networks Induced by Their Interaction with an Oppositely Charged Surfactant. Theory. *Macromol. Theory Simulations* **1992**, *1* (3), 105–118. https://doi.org/10.1002/mats.1992.040010301.

(31) Yin, D. W.; Olvera De La Cruz, M.; De Pablo, J. J. Swelling and Collapse of Polyelectrolyte Gels in Equilibrium with Monovalent and Divalent Electrolyte Solutions. *J. Chem. Phys.* **2009**, *131* (19). https://doi.org/10.1063/1.3264950.

(32) Kamcev, J.; Paul, D. R.; Freeman, B. D. Ion Activity Coefficients in Ion Exchange Polymers: Applicability of Manning's Counterion Condensation Theory. *Macromolecules* **2015**, *48* (21), 8011–8024. https://doi.org/10.1021/acs.macromol.5b01654.

(33) Kamcev, J.; Galizia, M.; Benedetti, F. M.; Jang, E. S.; Paul, D. R.; Freeman, B. D.; Manning, G. S. Partitioning of Mobile Ions between Ion Exchange Polymers and Aqueous Salt Solutions: Importance of Counter-Ion Condensation. *Phys. Chem. Chem. Phys.* **2016**, *18* (8), 6021–6031. https://doi.org/10.1039/c5cp06747b.

(34) Kamcev, J.; Paul, D. R.; Manning, G. S.; Freeman, B. D. Predicting Salt Permeability Coefficients in Highly Swollen, Highly Charged Ion Exchange Membranes. *ACS Appl. Mater. Interfaces* **2017**, *9* (4), 4044–4056. https://doi.org/10.1021/acsami.6b14902.

(35) Kamcev, J.; Paul, D. R.; Freeman, B. D. Effect of Fixed Charge Group Concentration on Equilibrium Ion Sorption in Ion Exchange Membranes. *J. Mater. Chem. A* **2017**, *5* (9), 4638–4650. https://doi.org/10.1039/c6ta07954g.

(36) Kamcev, J.; Paul, D. R.; Freeman, B. D. Equilibrium Ion Partitioning between Aqueous Salt Solutions and Inhomogeneous Ion Exchange Membranes. *Desalination* **2018**, *446* (May), 31–41. https://doi.org/10.1016/j.desal.2018.08.018.

(37) Yu, C. J.; Ri, U. S.; Ri, G. C.; Kim, J. S. Revealing the Formation and Electrochemical Properties of Bis(Trifluoromethanesulfonyl)Imide Intercalated Graphite with First-Principles Calculations. *Phys. Chem. Chem. Phys.* **2018**, *20* (20), 14124–14132. https://doi.org/10.1039/c8cp01468j.

(38) Marcus, Y. The Standard Partial Molar Volumes of Ions in Solution. Part 4. Ionic Volumes in Water at 0-100 °C. *J. Phys. Chem. B* **2009**, *113*, 10285–10291. https://doi.org/10.1021/jp9027244.

(39) Newman, J.; Chapman, T. W. Restricted Diffusion in Binary Solutions. *AIChE J.* **1973**, *19* (2), 343–348. https://doi.org/10.1002/aic.690190220.